



Behavior of anchored walls in soils overlying rock in Stockholm

Jianqin Ma, Associate Professor, College of Highway, Chang'an University, Xi'an, China; email: majq@gl.chd.edu.cn

Bo Berggren, Vice director in general, Swedish Geotechnical Institute, Linköping, Sweden; email: bo.berggren@swedgeo.se

Per-Evert Bengtsson, Senior research and consultant engineer, Swedish Geotechnical Institute, Linköping; email: Swedenper-evert.bengtsson@swedgeo.se

Håkan Stille, Professor, Royal Institute of Technology (KTH), Stockholm, Sweden; email: Hakan.Stille@byv.kth.se

Staffan Hintze, Professor, Royal Institute of Technology (KTH), Stockholm, Sweden; e-mail: Staffan.Hintze@byv.kth.se

ABSTRACT: *The deformations of retained soil and retaining walls are of importance for the design of a deep excavation in soft soils. The beneficial influence of bedrock underlying the soils on the behavior of the retaining wall needs proper evaluation. This contribution shows a case study on deep excavation in soft soils overlying bedrock at the South Link tunnel project in Stockholm. The behaviors of sheet pile walls and retained soils at the South Link show that both lateral displacement and settlement are larger than the magnitude from similar case histories. Exemplified by a test section, the features of lateral displacement are analyzed with monitoring and PLAXIS simulating results. The analysis results indicate that the displacement mainly occurs during the upper excavations and that the beneficial influence of bedrock may be overshadowed by the low strength of soils where depth of the excavation bottom to bedrock is larger than the excavation depth.*

KEYWORDS: Behavior, sheet pile wall, deep excavation, soft soil, bedrock, Stockholm

SITE LOCATION: [IJGCH-database.kmz](#) (requires Google Earth)

INTRODUCTION

The idea of greater and more efficient use of underground space has been accepted since the 1970s. Deep excavations are being carried out to meet the surging need for infrastructure in urban areas. To control the movements of the adjacent ground during construction, a retaining wall system is often used to provide stability. In order to ensure a successful excavation, the behaviors of the wall and the adjacent ground must be considered during the design phase. However, soil movements due to excavations are not entirely predictable because they are related to a number of factors including soil type, base stability, compression and rebound of the soils, consolidation of soils, wall system stiffness, construction procedures, and workmanship. Any of these factors can contribute to the overall movement of a supported excavation. It is difficult to make a direct and quantitative analysis of the deformation of the ground and support system because the interaction of the factors is complex. So, the estimation of ground movements during excavations is generally a combination of analytical and empirical methods, judgment, and experience. Peck (1969), Mana, and Clough (1981); Clough and O'Rourke (1990); and Ou et al. (1993) provided well-accepted empirical analysis diagrams on this subject. Bjerrum et al. (1972), Hashash and Whittle (1996, 2002) and Finno and Calvello (2005) gave examples for numerical analysis. More recently, Shao and Macari (2008) reviewed the application of in situ instrumentation and numerical feedback analysis on deep excavations.

The deformation feature of the wall-prop system depends not only on the properties of the excavated soils, but also on the properties of the underlying layers. Mana and Clough (1981) considered the influence of a firm layer underlying soft soil strata using a parameter of "depth to an underlying firm layer." Recently, studies carried out on excavations in multilayered

Submitted: 15 October 2009; Published: 23 April 2010

Reference: Ma J., Berggren B., Bengtsson P-E., Stille H., Hintze S., (2010). *Behavior of anchored walls in soils overlying rock in Stockholm*. International Journal of Geotechnical Engineering Case Histories, <http://casehistories.geoengineer.org>, Vol.2, Issue 1, p.1-23. doi: 10.4417/IJGCH-02-01-01.



soil deposits overlying rock stratum (Wong et al., 1997; Yoo, 2001; and Long, 2001) showed that both the lateral and vertical deformations are less than those in soil deposits without underlying bedrock. This implies that the design practice, based on traditional empirical results, may be somewhat conservative. However, the studies also show that the deformation features are of regional characteristic. There are great differences in deformation magnitude between the case histories, such as from Korea (Yoo, 2001), Singapore (Wong et al., 1997), Oslo (Long, 2001), and Taipei (Ou et al., 1993). Therefore, whether the results of previous studies are applicable to in situ walls in multilayered soils overlying rock in Stockholm is of interest.

This study aims at understanding the behavior of in situ anchored steel sheet pile walls constructed mainly in soft soils overlying bedrock. This situation is frequently encountered in the urban areas of Sweden. To meet this goal, measured data from the contractor of South Link 10 (SL10), which is a part of a tunnel system in south Stockholm, are analyzed. Particular emphasis has been placed on the beneficial influence of bedrock on the retaining wall deformation. A 2D finite element analysis on a test section is used to provide insights into the influence of bedrock.

PROJECT DESCRIPTION

The South Link tunnel system in Stockholm is the largest city tunnel in Europe. SL10, the west part of the system (fig. 1), comprises a 460 m long underground structure including 40 m of rock tunnel, a cut and cover concrete tunnel, and tunnel ramps. The coordinates of the project are 59.337742, 18.062897. The tunnel system was open to use in 2004. The tunnel complex handles over 60,000 vehicles per day.

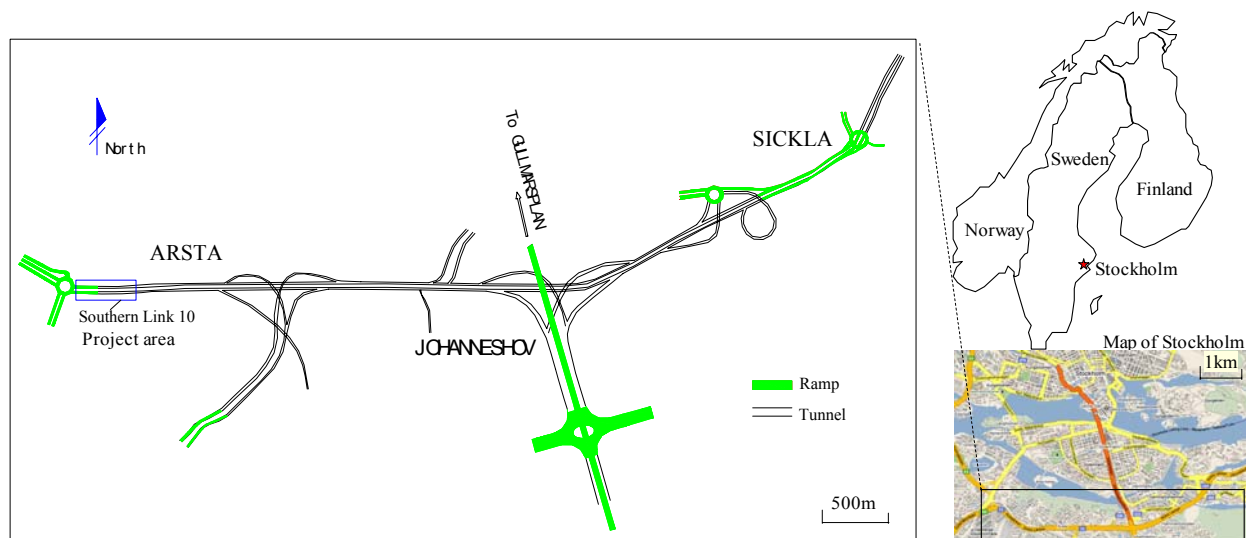


Figure 1. SL10 is a part of the Södra Länken tunnel system in Stockholm.

Geotechnical Conditions

The geotechnical conditions can be simply expressed as soils overlying bedrock. A longitude geotechnical profile at SL10 is shown in Figure 2. The soils consist of a fill deposit overlying a sequence of glacial deposits, mainly composed of soft clay. There is a layer of about 1 m desiccated dry crust of organic soil underlying the fill. The clay has an organic content of about 5% just under the crust, which decreases with depth and is less than 2% from about 6 m depth and downwards. The natural water content is about equal to the liquid limit and decreases from a maximum of about 130% to about 70% in the bottom layers. The bulk density increases from 1.3 kN/m³ to 18 kN/m³ at the bottom.

Thin layers of silt and sand are present in the soft clay. At the bottom of the soils, there is granular soil or dense moraine about 1 m thick. In some areas, the granular soil is missing. The bedrock is gneiss with a surface layer that is, for the most part, unweathered. The elevation of the surface varies within the working area (Fig. 2). The soil strata reach their maximum depth of approximately 25 meters in the central part of the project. Groundwater level is around 1 to 2 m below the surface. The pore water pressure in the ground is hydrostatic.



The shear strength values in the natural ground were mainly determined by field vane tests. The measured values have been corrected according to the recommendation by Larsson et al. (1984) and as shown by Bergdahl et al. (2003). The undrained shear strength of the clay is around 16 kN/m^2 , with an increase of 2 kN/m^2 per meter below the level of $+10 \text{ m}$ in the local elevation system. The ground surface level at deep excavations is around $+15 \text{ m}$ (Fig. 2). The soil in the upper two metres is slightly overconsolidated due to the dry crust effect. The overconsolidation ratio (OCR) of the clay decreases from about 1.4 at the surface to 1.0 at a level of $+6 \text{ m}$ and below (Hintze et al., 2000). The generalized geotechnical conditions at various excavations are presented in Figure 3.

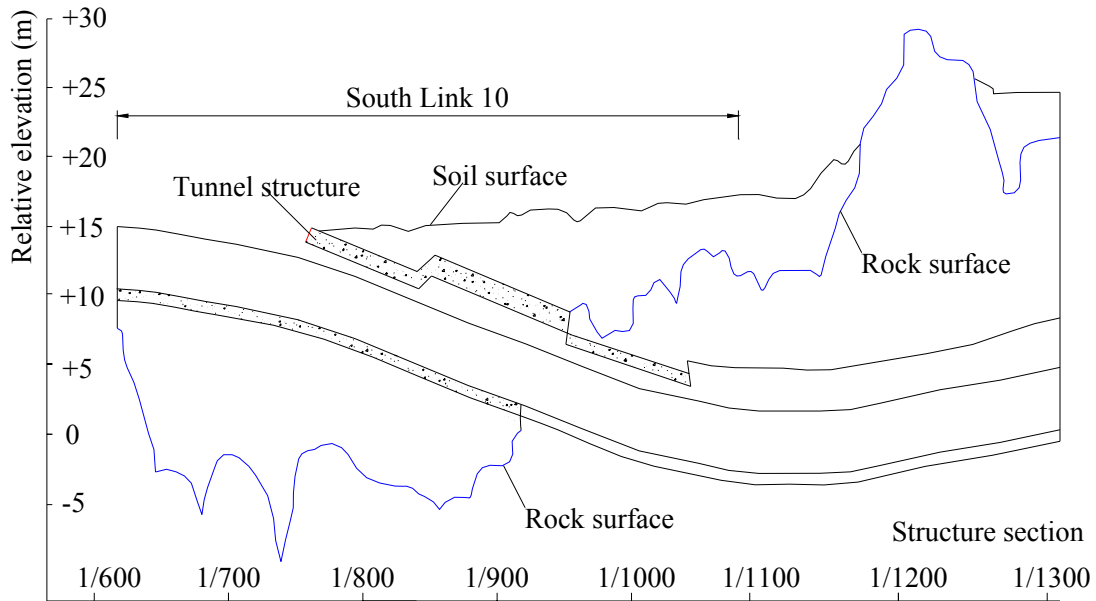


Figure 2. Longitudinal section of SL10 showing structures and geotechnical layers.

	Description	Water content (%)	Unit weight (kN/m^3)	Undrained shear strength	Overconsolidation ratio (OCR)
15	Fill	20 40 60 80 100 120	12 14 16 18	10 15 20 25 30 35 40 (kPa)	0.8 1.0 1.2 1.4 1.6
14	Dry crust				
13	Green and gray clay				
12	Green and gray clay				
11	Dark gray clay				
10	Dark gray clay				
9	Black clay				
8	Black clay				
7	Dark gray clay				
6	Dark gray clay				
5	Gray clay				
4	Gray clay				
3	Gray varved clay				
2	Gray varved clay				
1	Gray varved clay				
0	Gray varved clay				
-1	Gray varved clay				
-2	Sand				
-3	Rock				

Figure 3. Generalized geotechnical conditions at a typical excavation.



Sheet Pile Walls and Anchors

The deep excavation area of SL10 is 3 m to 16 m in depth and 40 m to 50 m in width. Sheet pile walls with back-tied anchors were used to meet the requirement of the construction works close to buildings and heavy traffic. LX32 type sheet pile was driven into the bedrock. The flexural stiffness of the sheet pile wall is $151 \text{ MNm}^2/\text{m}$. Dyform $7\phi 15.2 \text{ mm}$ or $9\phi 15.2 \text{ mm}$ type anchors, with inclination angles of 30° , 35° , or 45° , were keyed into the bedrock. The connection between the sheet piles and the bedrock were sealed by grouting to prevent groundwater leakage and to reduce settlements (Hintze et al., 2000).

Both the length of the wall and the number of anchors vary because the excavation depth and the thickness of soils vary throughout the project. The number of anchors in a section is accordingly one to eight. The vertical and horizontal intervals of anchors vary from 1.5 m to 3.0 m and from around 1.0 m to more than 3.0 m, respectively.

Excavation Procedures

The sequence of construction activities at the site consists of wall installation, excavation, and support. The sheet pile walls are installed before excavation. The installation is followed by grouting at the toe of the sheet piles walls. Excavations inside the sheet pile walls are proceeded in stages, which are alternated by the installation and preloading of anchors. Excavation and anchor installation in section 1/840N is exemplified in Figure 4, in which the excavations are presented as excavations I through VI from surface to formation level. For excavations I through V, each excavation stage is followed by a stage of anchor installation and preloading of anchors.

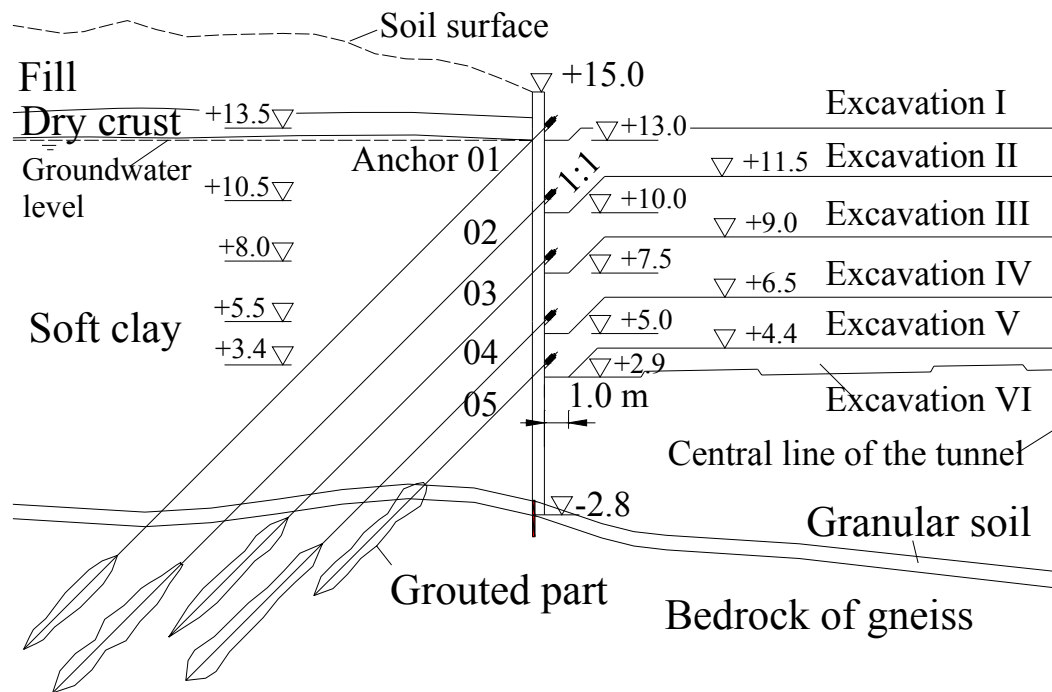


Figure 4. Excavation and anchor installation in section 1/840N.

Monitoring Instruments

Figure 5 shows the plan of the locations of instrumentations, including 11 inclinometers and 11 settlement points. For section 1/840N, 3 anchor load cells and 3 groundwater table wells around the section are also illustrated. The inclinometers are mostly 2.0 m from the sheet pile wall and the settlement points are 1.0 m from the wall. Inclinometers, with their toes keyed into bedrock, are vertically installed. The interval of the sensors in an inclinometer is 2.0 m and its toe is considered totally fixed in displacement calculation. Typically, a complete set of instrument readings was obtained every day when excavation occurred around the test sections.

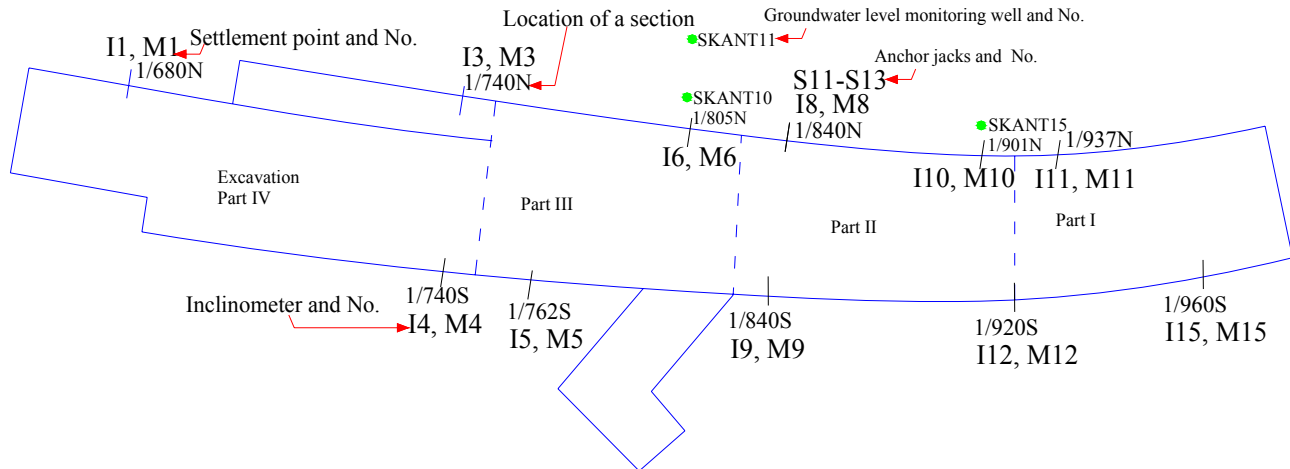


Figure 5. Plan showing locations of monitoring instruments.

FEATURES OF MOVEMENT

Data from SL10

The data from SL10 is tabulated in Table 1. Parameters include thickness of soil layer, excavation depth, average vertical anchor support spacing, maximum lateral displacement, and settlement.

Table 1. Data of the deep excavations at South Link 10 in Stockholm.

Section	Thickness of soil layer (m)	Excavation depth (m)	h_{avg} * (m)	$\delta_{h,m}$ ** (mm)	$\delta_{v,m}$ *** (mm)
1/680N	17.4	3.1	1.60	19	/
1/740N	23.3	6.7	2.60	77	75
1/740S	21.5	7.5	2.10	95	78
1/762S	22.7	8.3	2.39	62	68
1/805N	18.9	10.3	2.20	48	64
1/840N	17.8	12.1	1.70	106	148
1/840S	20.2	10.0	1.94	169	210
1/900N	16.2	14.4	2.68	150	379
1/920S	16.6	14.9	1.87	97	188
1/937N	16.0	5.6	/	23	/
1/960S	/	/	/	16	46

* h_{avg} - Anchor support vertical spacing (average).

** $\delta_{h,m}$ - Maximum lateral displacement.

*** $\delta_{v,m}$ - Maximum settlement

Magnitude of Movement

General Pattern

The general features of retaining wall lateral displacement from several test sections are shown in Figure 6. Originally used by Peck (1969), this is a common way to measure the maximum lateral displacement as a value in relation to the excavation depth (H) as well as the maximum settlement. The maximum lateral displacement and settlement data from SL10 versus excavation depth H are plotted in Figure 7(a) and 7(b), respectively.

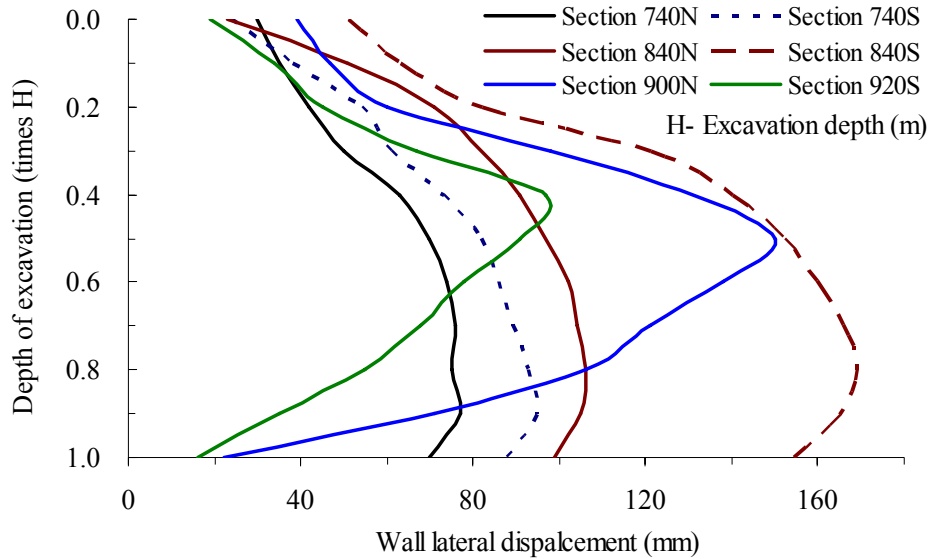


Figure 6. General features of retaining wall lateral displacement.

Figure 7(a) shows that the maximum lateral displacement is between 0.4% H and 1.7% H, and tends toward 1% H. Figure 7(b) shows that the maximum settlement is between 0.6% H and 2.7% H, and tends toward 1.5% H. The magnitude of the settlement is larger than that of the lateral displacement at SL10.

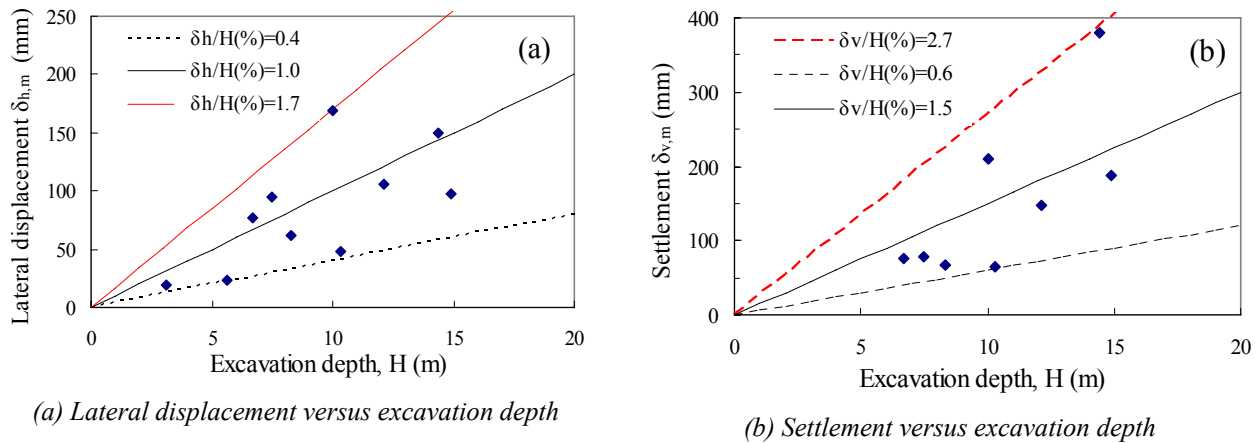


Figure 7. Maximum deformation versus excavation depth.

Relationship between Lateral Displacement and Settlement

For well-constructed excavations, the magnitude of the ground's lateral and vertical movements are correlated. In order to show the relationship between the maximum lateral displacement and settlement, data in Table 1 are plotted in Figure 8. Figure 8 shows that the magnitude of the maximum lateral displacement is about 0.4 to 1.25 times that of the maximum settlement in SL10. This indicates that the magnitude of the maximum settlement is partially different from the general pattern, which shows that the maximum lateral and vertical movements are of the same order of magnitude (Goldberg et al., 1976; Mana and Clough, 1981; Clough and O'Rourke, 1990; Long, 2001; and Moormann, 2004).

The magnitude of the ground movements associated with excavation support has typically been categorized according to the predominant soil type in which the excavation is made. To compare to the database, which was categorized into five sets in Long (2001), the SL10 data is shown in Figure 9. In Figure 9, four sets of Long (2001) are quoted as follows:



1. Propped walls, with the thickness of the soft soil layer (h) less than $0.6H$ of the excavation depth (shown as: $h < 0.6H$ in Figure 9(a));
2. Propped walls, with the thickness of the soft soil layer (h) larger than $0.6H$ of the excavation depth and stiff soil at dredged level (shown as: $h > 0.6H$, stiff soil at dredge in Figure 9(a));
3. Propped walls, with the thickness of soft soil layer (h) more than $0.6H$ of excavation depth and soft soil at dredge level (shown as: $h > H$ in Figure 9);
4. Low factor of safety against base heave (shown as: Low FOS against base heave in Figure 9).

Figure 9(a) shows that both lateral and vertical movements at SL10 are far larger than those of the data from propped walls with $h < 0.6H$. The magnitude of the displacement data from $h > 0.6H$ with stiff soil at dredged level is somewhat larger than that of the data from propped walls with $h < 0.6H$, but most of them are less than those from SL10.

Figure 9(b) shows that the magnitude of the data of $h > H$ covers almost all the data from SL10. This indicates that the data from the deformation of SL10 is, to some extent, similar to the data of Long (2001) relating to the situation of soft soil at dredged level.

The data from the set of low FOS against base heave is almost in the same range as the data from SL10, which lies between the lines of $\delta_{h,m}/\delta_{v,m} = 1.25$ and $\delta_{h,m}/\delta_{v,m} = 0.4$. However, two points of both lateral and vertical displacement are larger than 300 mm, which is much larger than the displacement data from SL10. Regarding the geotechnical condition, SL10 is more similar to that of the $h > H$ in Long (2001).

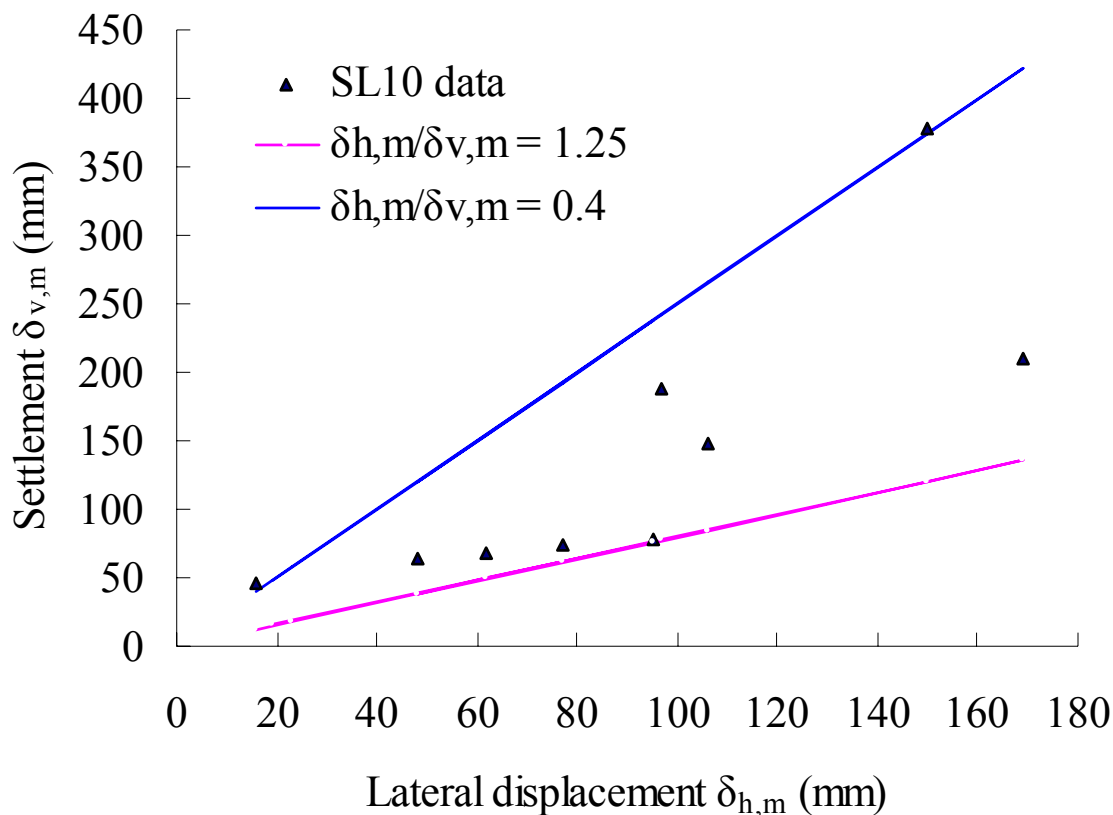


Figure 8. Maximum lateral displacement versus settlement.

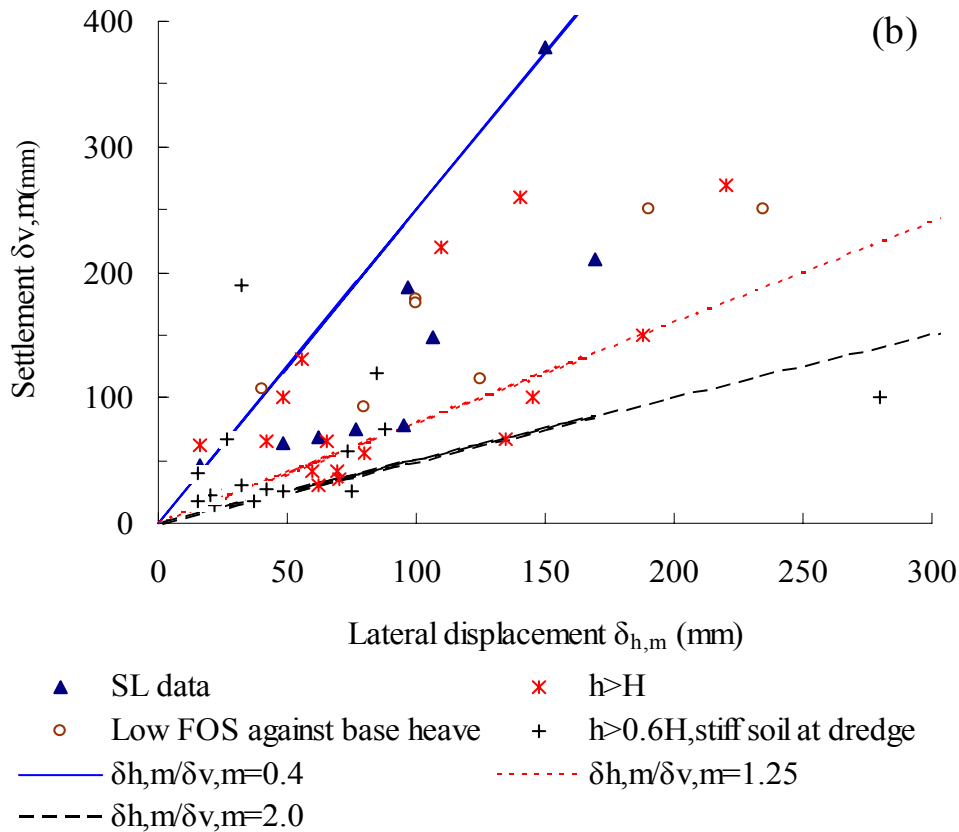
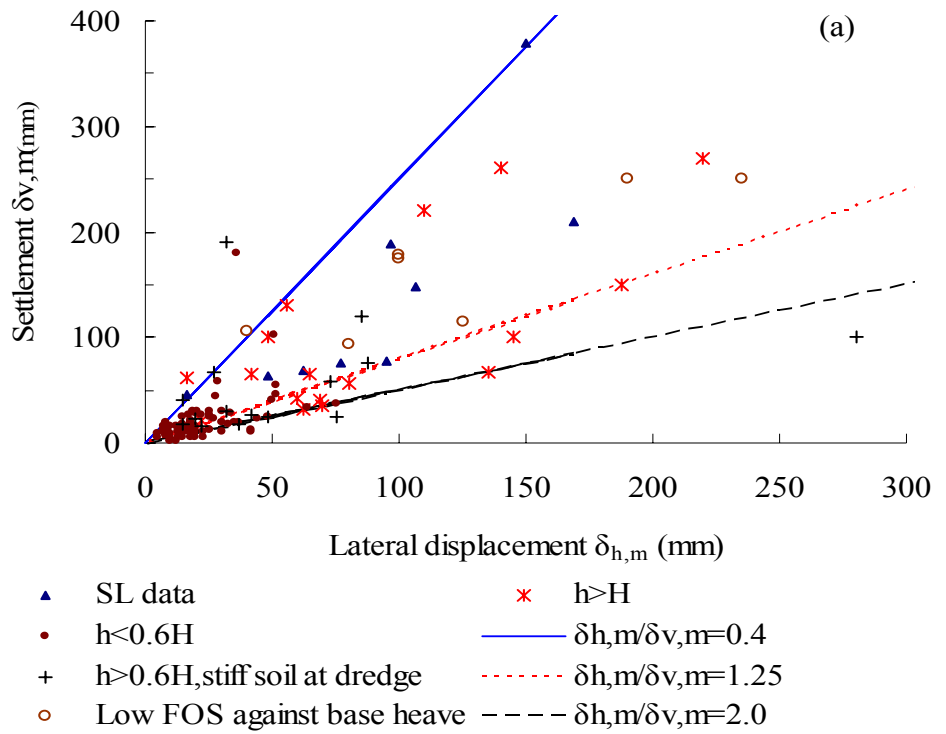


Figure 9. Maximum lateral displacement versus maximum settlement.



FEATURE OF LATERAL DISPLACEMENT IN SECTION 1/840N

Monitoring Results

Increment for Excavation Stages

In section 1/840N (Fig. 4), monitoring instruments began after anchor 01 was preloaded. Monitored results show that the lateral displacement is mainly related to excavation activities, shown as excavations I through VI in Figure 4. For excavations II through VI, the increments of lateral displacement are shown in Figure 10. Figure 10 shows that most of the lateral displacement increment takes place in excavations II, III, and IV, and a quick increase occurs at the end of excavation III. In excavation IV, the increment occurs mainly in the lower part of the test section. In excavation V and VI, the lateral displacement increment is small or even negative. When the excavation depth increases, the change of the increment pattern from excavation III to IV corresponds to the decrease tendency of the elevation of the maximum lateral displacement points.

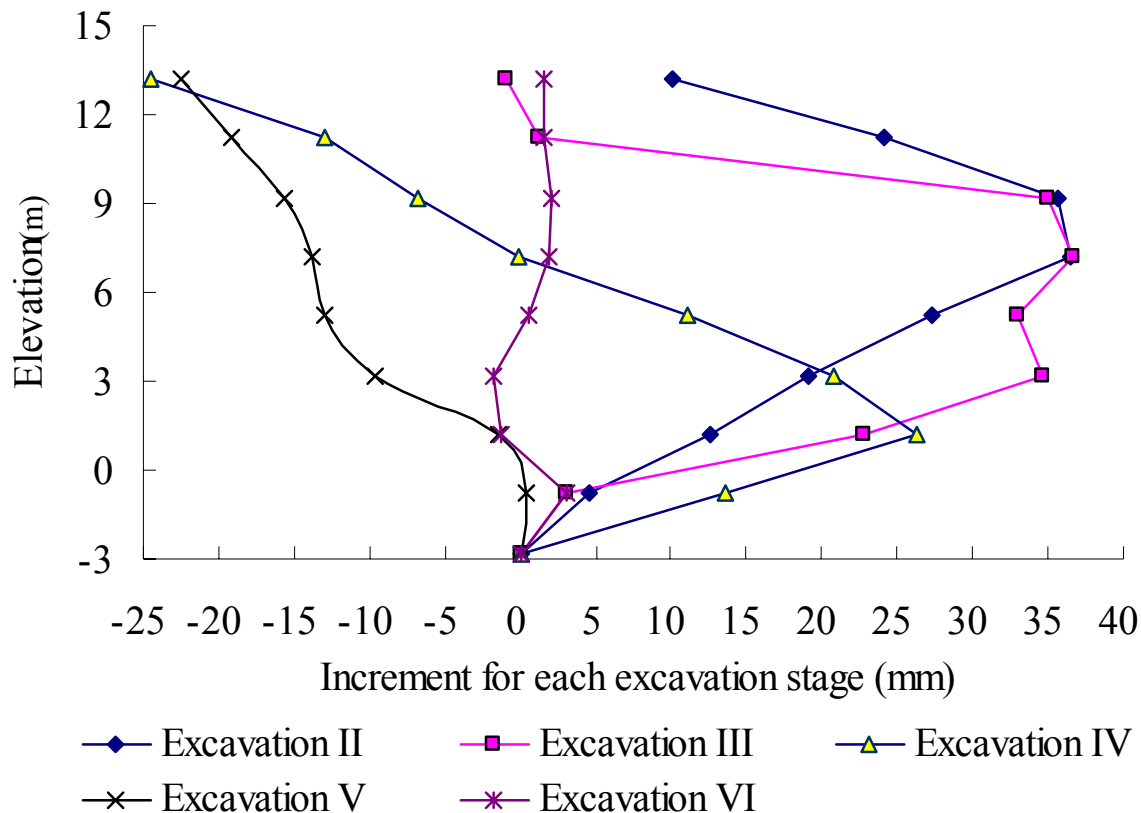


Figure 10. Lateral displacement increment for excavation stages.

During construction, excavations inside the sheet pile walls were proceeded in stages, which were alternated by the installation and preloading of anchors. In practice, the magnitudes of the preload of anchors 01 and 02 (Fig. 4) decreased with excavation. After excavation III, anchors 01 and 02 were re-preloaded to meet their designed preload magnitudes to control the ground movement. As a result, the displacement of the upper part of the wall was greatly affected by the preload. During excavations IV and V, the lateral displacement increments in the upper part were negative, with the maximum magnitude reaching 35mm. This pushing back effect of the wall is related to the re-preloading of anchors 01 and 02 (Fig. 4) and their re-preloaded stresses being well maintained.

Figure 11 shows the elevation of the maximum lateral displacement points and their increment magnitude in excavation stages. In general, both the increment and the elevation of the points decrease from excavation II through VI.

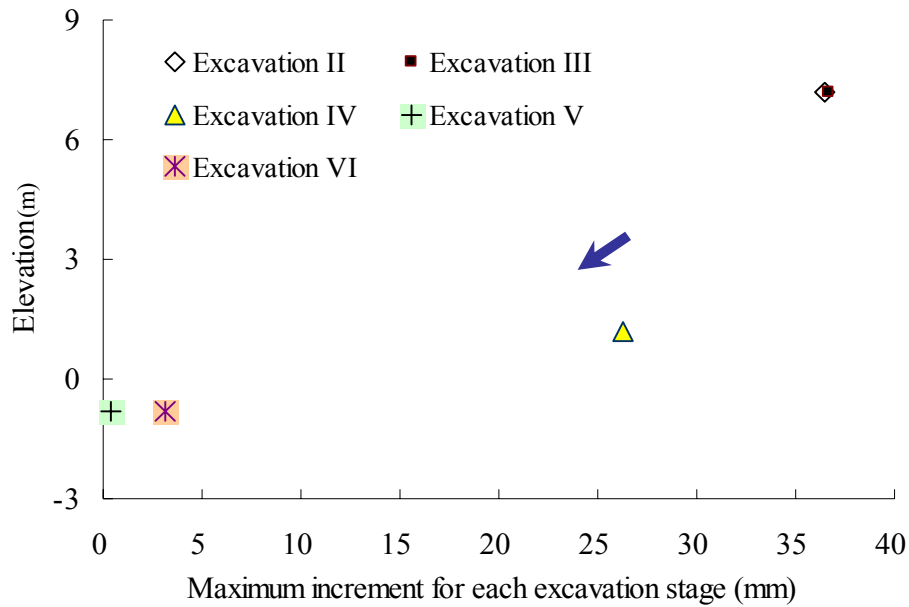


Figure 11. Elevation of the maximum displacement increment point for excavations.

Increment with Excavation Depth.

In general, the depth of the maximum lateral displacement increment point in excavation stages increases with excavation depth, as shown by the correlation line in Figure 12. The maximum increment point is about 3 m below the bottom of excavation in a stage. However, there is no simple relationship between them. From excavation II to III, there is no increase of the depth of the maximum lateral increment point, while from excavation III to IV, a significant increase occurs. In excavation V, the increment of the depth of the maximum lateral increment point is almost the same as the increment of excavation depth. In excavation VI, there is no increment of the depth of the maximum lateral increment point. The difference of the increments of excavation depth and the depth of the maximum lateral increment point is clear in Figure 13. The increments of excavation depth are about two meters for each excavation. But there is no increase in depth for the maximum lateral increment point in excavations III and VI.

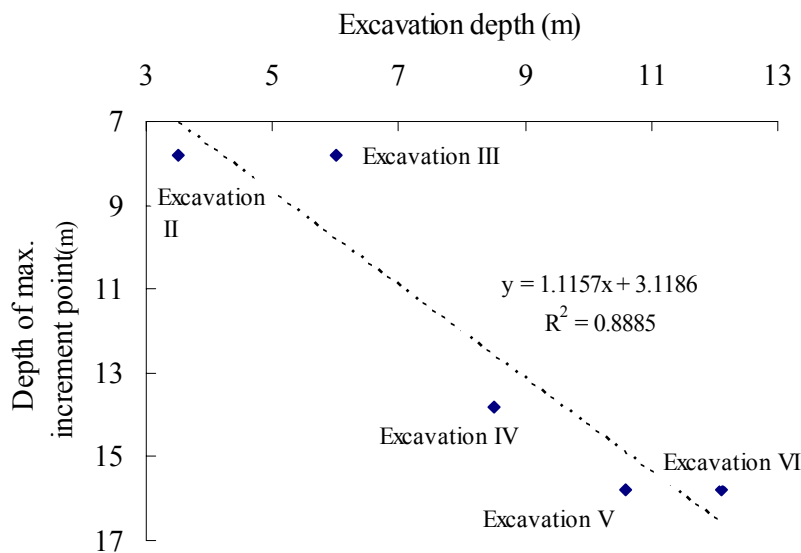


Figure 12. Correlation between the depths of the maximum increment point and excavation.

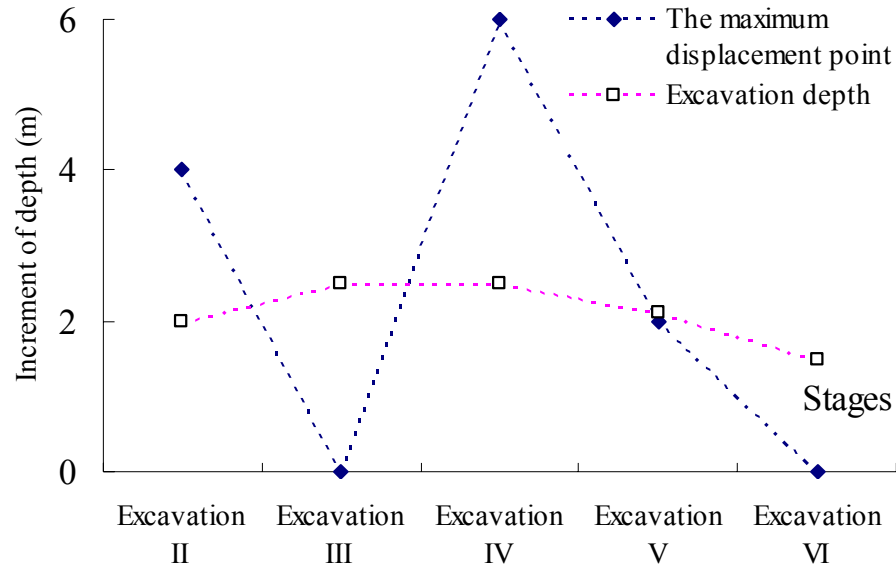


Figure 13. Depth increment of the maximum displacement point and excavation bottom

Analysis with PLAXIS

A 2D finite element analysis with PLAXIS code on section 1/840N was used to provide insights regarding the influence of bedrock and other parameters on the performance of an anchor back-tied wall system. The details of the numerical analysis were shown by Ma et al. (2006).

Model Description

A Mohr-Coulomb model is used and the excavation process is simplified as a symmetrical problem. The model includes a representation of the five distinct geotechnical layers, the sheet pile wall and anchor system, the construction stages, and the distribution loading on the surface. The model is 101.5 m wide and 25 m high. A 15-node triangular element is chosen to yield an accurate calculation (Brinkgreve, 2002). Standard fixities are used as model boundaries. Everything except wall installation (6 soil excavations, 5 anchor preloading stages, and 7 consolidation analysis stages) is presented in the model. Anchor installation is included in its preceding excavation stage while the preloading of an anchor is simulated as a separate stage. The wall installation is assumed “wished in place,” but the shear strength of the retained soil can only be 67% mobilized along the soil-wall interface. The general information of the analysis model is shown in Figure 14.

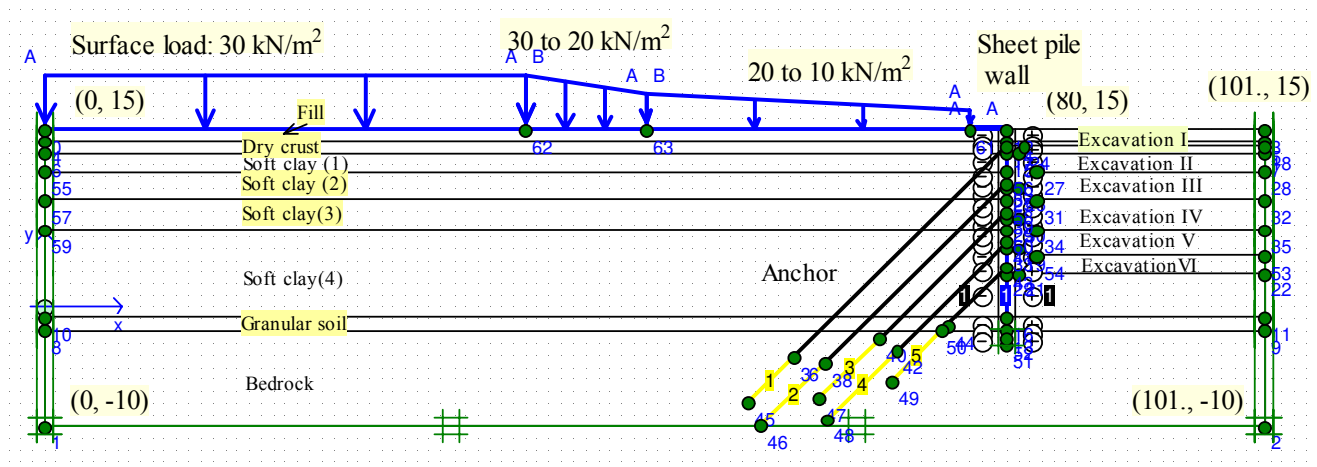


Figure 14. General overview of finite element analysis model. (A) General description and surface load.



Over a distance of 3 m, starting at the sheet pile wall, the distributed load is 10 kN/m^2 . From a distance of 3 m to 30 m away from the sheet pile wall, the distribution load is trapezoidal and varies from 10 to 20 kN/m^2 . From a distance of 30 m to 40 m away from the sheet pile wall, the distribution load is trapezoidal and varies from 20 to 30 kN/m^2 . From 80 m to 40 m away from the sheet pile, the distribution load is equal to 30 kN/m^2 .

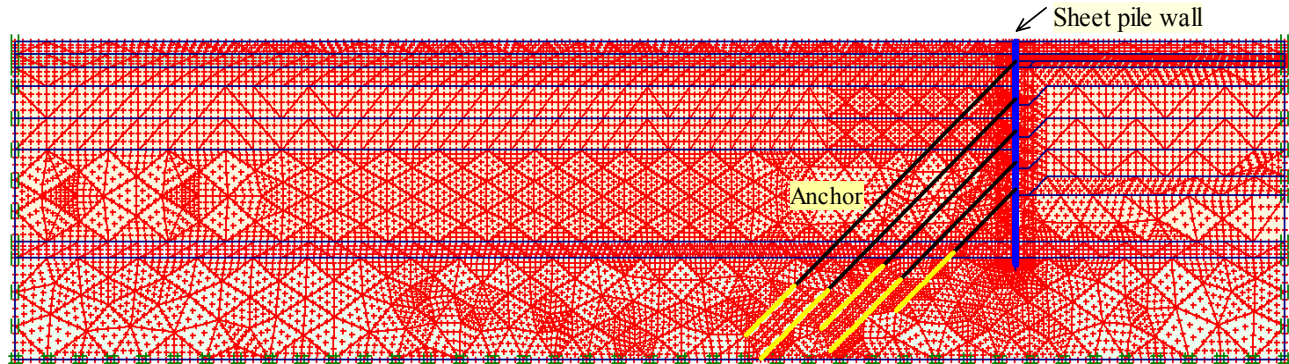


Figure 14. General overview of finite element analysis model. (B) Element distribution of mesh and the positions of anchors.

All five distinct geotechnical layers are simplified as horizontal in occurrence. From +15 m to +14 m there is a fill of loose fine soil, which is underlain by 1.0 m thick dry crust. The soft clay is 13.8 m thick. The surface of the bedrock is at -2.8 m. Groundwater level is 2.0 m below the surface. The water level is updated according to the monitoring results of SKANT 10, 11, and 15 (Fig. 5) during excavations. With the effect of soil overconsolidation on the lateral coefficient considered (Mayne and Kulhawy, 1982), the lateral coefficient value of k_0 is given from 1.38 to 1.0 from surface to the elevation of +6 m (Fig. 3).

The Young's modulus, cohesion strength, friction angle, and permeability coefficient of the geotechnical materials for the numerical model are shown in Table 2. The geotechnical parameters of the soils in numerical analysis are approximated mainly according to shear strength in practice. With a factor of safety being considered for a project, the Young's modulus of the soils are approximated as $250 c_u$ (Larsson, 1986; Larsson and Mulabdić, 1991), where c_u is undrained shear strength of soil. For the soft clay, the cohesion strength increment is 2 kN/m^2 per meter and the Young's modulus increment is 1600 kN/m^2 per meter with vertical reference elevation level at 10 m in the numerical model. The bedrock is considered to be an elastic material extending to large depth.

Table 2. Geotechnical parameters of the numerical model.

Parameter	Friction angle ($^\circ$)	Cohesion (kN/m^2)	Young's modulus (kN/m^2)	Permeability (m/day)
Fill	35	1.0	6000	1.0
Dry crust	0	30.0	15000	0.0001
Soft clay*	0	16.0	4900	0.0001
Till	38	0.5	35000	0.1
Bedrock	45	200	2000000	0.00001

* For the soft clay, the cohesion strength increment is 2 kN/m^2 per meter, and the Young's modulus increment is 1600 kN/m^2 per meter with a vertical reference elevation level of 10 m in the numerical model.

A surface load is given as varying from 30 kN/m^2 to 10 kN/m^2 on the left side of the excavation, according to the landform feature left to the excavation at section 1/840N (Fig. 4), as shown in Figure 14. The weight of the geotechnical materials above the elevation level +15 m is considered as a surface load. The surface load of 10 kN/m^2 is given to represent temporary traffic load during construction.

The sheet pile wall is 17.5 m long and its toe is totally fixed into rock. Its normal stiffness and flexural rigidity are $5 \times 10^6 \text{ kN/m}$ and $151259 \text{ kNm}^2/\text{m}$, respectively. The anchor data is given according to design parameters (Hintze et al., 2000).



Anchors are inclined at an angle of 45° . The maximum force of the anchor rod is 1.0×10^{15} kN and the normal stiffness of the geogrid is 1.0×10^8 kN/m. The preloads of the anchors are given according to monitoring results (Ma et al., 2006).

Comparison between Numerical and Monitoring Results

In section 1/840N, an inclinometer was put into usage after the anchor 01 (Fig. 4) was preloaded. The lateral displacement related to the excavation I and the anchor 01 preloading was only partially instrumented in practice. The monitored results show that the lateral displacement at the test section is mainly related to excavation activities. In order to show the lateral displacement in accordance to the practical value, the lateral displacement due to the excavation I is approximated with the corresponding analysis result for the excavation I. The lateral displacement related to excavation I is considered to be the same as that of the analysis. The effect of the reference points of the numerical analysis and monitoring results is checked by the comparison between the first monitoring and numerical result before excavation II, as shown in Figure 15. The difference between analysis and monitoring results is insignificant. Compared to the lateral displacement profile, the characteristic of cantilever deformation is more typical for the numerical result than for the monitoring behavior. For the lower part of the sheet pile wall, the monitored displacements are larger than those calculated. In practice, the wall deforms as an ideal elastic beam with its toe totally fixed.

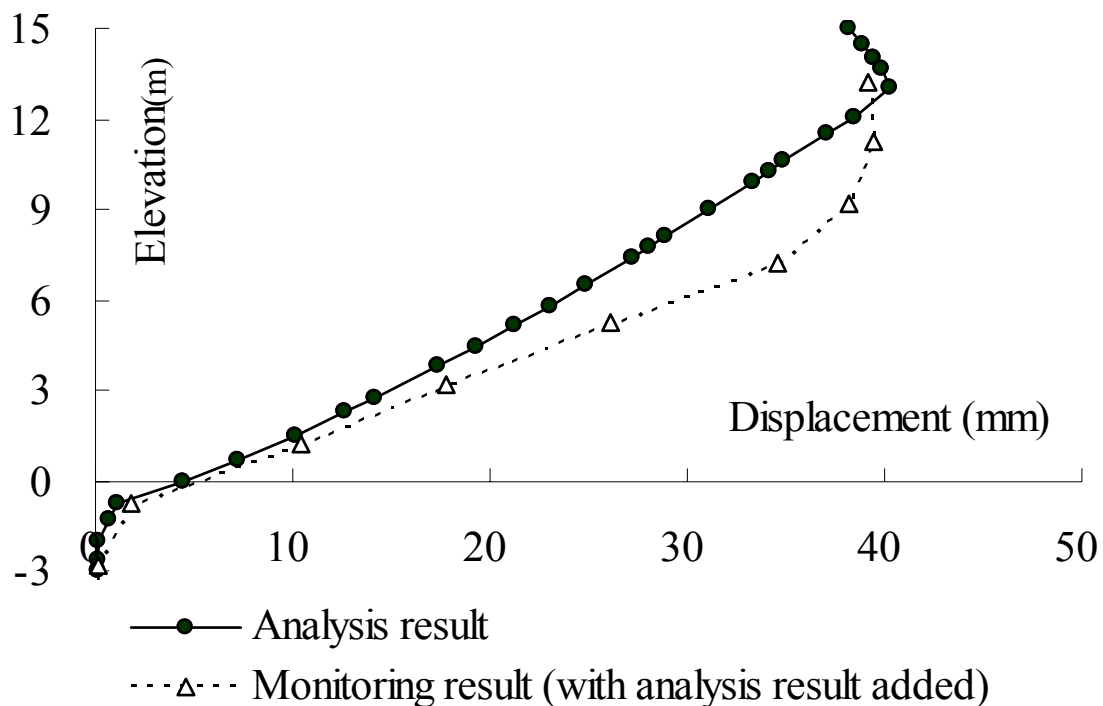
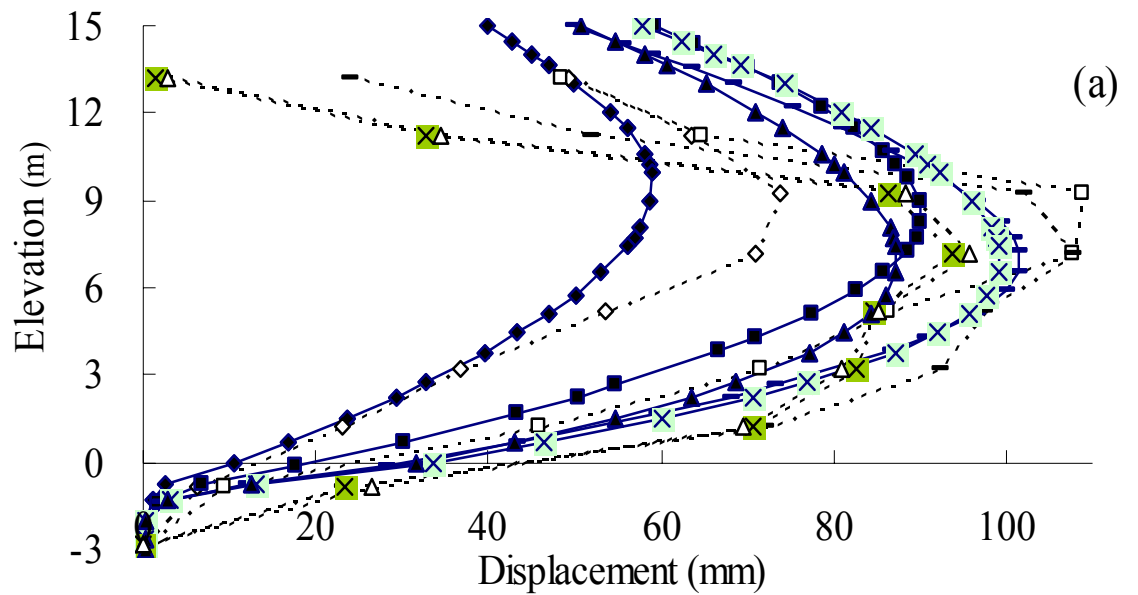


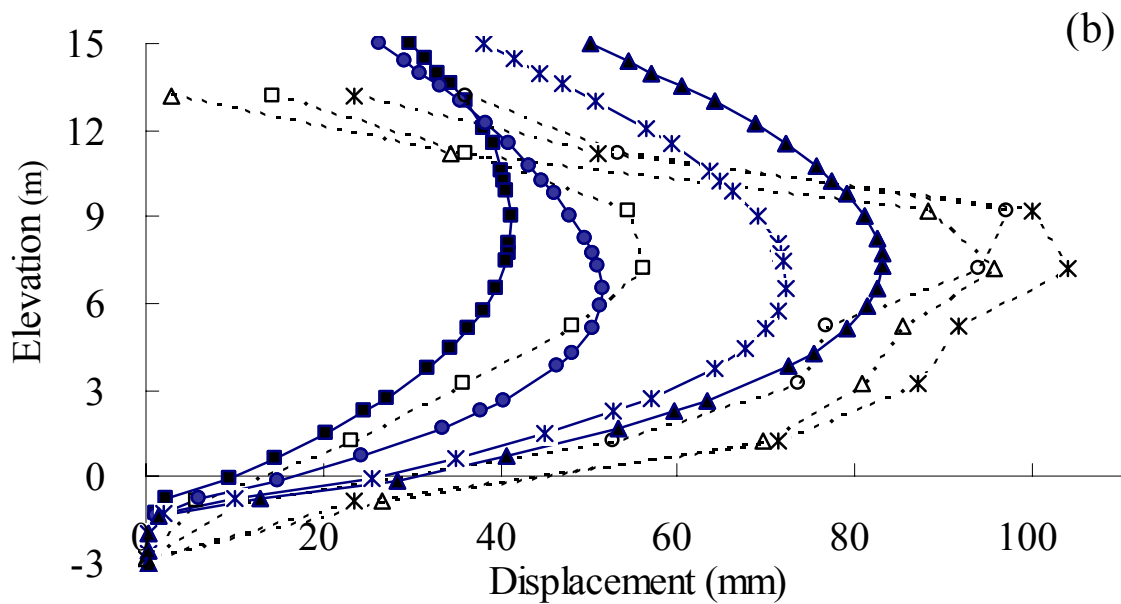
Figure 15. Comparison of analysis and monitoring displacements.

Numerical analysis results for other stages are compared with corresponding monitoring values in Figure 16. Figure 17 shows the comparison between the elevations of the maximum lateral displacement points of the analysis and monitoring results. In Figures 16 and 17, the difference between the analysis and monitoring results is not significant except in the upper part. The magnitude of the monitoring and analysis results can be generally considered similar, especially for the excavation stages with the lateral large displacement increase.

Figure 16 shows that the difference between the numerical analysis and monitoring results is less in the lower part of the test section than in the middle and upper parts. The larger difference between the numerical analysis and monitoring results in the upper part of the test section indicates the influence of other factors, such as surface load and anchor preloads (Ma et al., 2006). The smaller difference between the numerical analysis and monitoring results in the lower test section implies that the influence of the bedrock on the lateral displacement is significant where excavation approaches the bedrock.



- ◆— A-Stage 4 - - -◇- - - M-Stage 4 —■— A-Stage 6 - - -□- - - M-Stage 6
- ▲— A-Stage 8 - - -— M-Stage 8 —×— A-Stage 10 - - -×- - - M-Stage 10
- ▲— A-Stage 12 - - -△- - - M-Stage 12



- A-Stage 5 - - -□- - - M-Stage 5 —●— A-Stage 7 - - -○- - - M-Stage 7
- ×— A-Stage 9 - - -×- - - M-Stage 9 —▲— A-Stage 11 - - -△- - - M-Stage 11

* The prefixes "A-" and "M-" denote the results of numerical analysis and monitoring, respectively.

Figure 16. Lateral displacements of analysis and monitoring in stages.

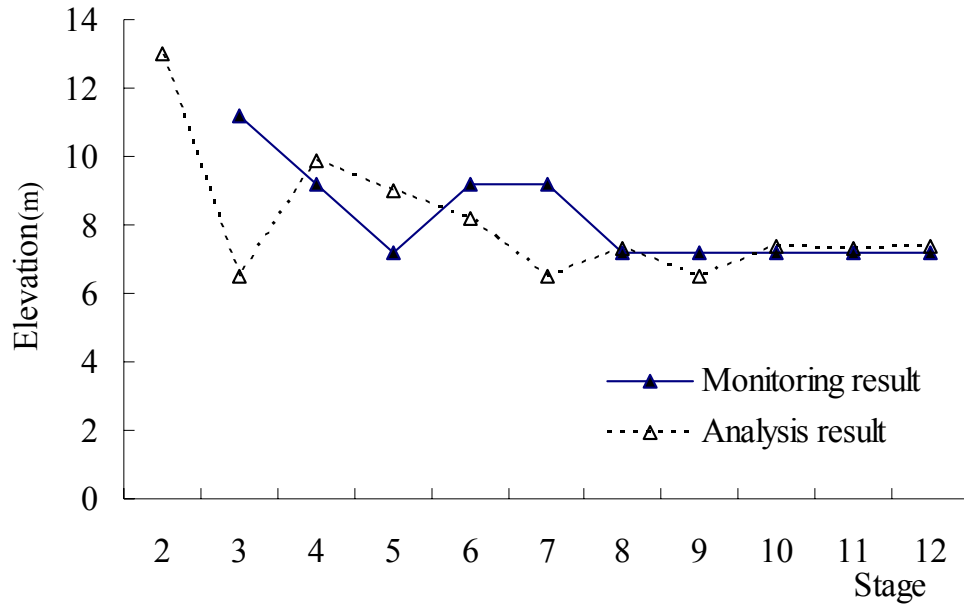


Figure 17. Elevation of the maximum displacement points in stages.

DISCUSSION OF THE FACTORS OF CONTROLLING LATERAL DISPLACEMENT

Effect of Bedrock

The studies on deep excavations in soft clay overlying a stiff soil layer or bedrock show that stiff layers could have a dominating influence on the behavior of a propped wall system (Mana and Clough, 1981; Wong et al., 1997; Yoo, 2001; and Long, 2001). Yoo (2001) made a conclusion regarding deep excavation in soft soil overlying rock in Korea, which is, to some extent, similar to SL10 in geological setting. The data from Yoo (2001) includes research on a variety of wall types; namely, diaphragm walls, sheet pile walls and H-pile walls, soil cement walls, and cast-in-place walls. The sheet pile walls and H-pile walls generally have a larger lateral displacement than the others (Yoo, 2001). Data relevant to sheet pile walls and H-pile walls from Yoo (2001), Long (2001), and SL10, are shown in Figure 18 in terms of excavation depth versus normalized lateral displacement $0.1\delta_{h,m}/H$, where $\delta_{h,m}$ is the maximum lateral displacement in millimeters and H is depth of excavation in meters. Figure 18 shows that all of the data from Korea (Yoo, 2001) are below the ratio 0.6 of $0.1\delta_{h,m}/H$, while the data from SL10 is above this ratio. This implies that the influence of the bedrock on the displacement of the SL10 should not be an exclusive factor, and that the displacement feature in the Stockholm area is far different from that of Korea.

Figure 18 shows that the maximum lateral displacement magnitude is more similar to the data from Long (2001), excluding two points, than to the data from Yoo (2001). The similarity between the displacement features of SL10 and the propped walls with $h>H$ from Long (2001) indicates that the relative thickness of the soft soil layer could have a significant influence on the deformation of the anchored sheet pile walls.

Data from SL10 and Long (2001) are plotted in Figure 19 in terms of H/h versus $0.1\delta_{h,m}/H$. Figure 19 shows that the normalized maximum lateral displacement increases with decreasing H/h . This means that the maximum lateral deformation magnitude increases with the formation level more above the bedrock or stiff layer.

Figures 18 and 19 indicate that the influence of the bedrock could be overshadowed by a low ratio of H/h , provided that the deep excavation formation level does not reach the bedrock or that the ratio of H/h is less than 1.0, as shown in SL10. In order to check this deduction, the normalized lateral displacement with excavation stages in section 1/840N is shown in Figure 20 in terms of the ratio of excavation depth to soil thickness. Figure 20 shows that the normalized lateral displacement increases from excavation II to III and then decreases, almost in a linear manner, with increasing excavation depth. This indicates that the influence of the bedrock on the lateral displacement increases as the excavation bottom approaches to bedrock.



For section 1/840N, large increments of lateral displacement take place in excavations II and III (Figs. 10 and 11). The ratio of the depth from excavation bottom to bedrock (D) and excavation depth (H) are given in Figure 21. In general, the maximum lateral displacement increment for excavation decreases as the ratio of D/H decreases. Figure 21 shows that the increments in excavations V and VI are small. In excavation IV, the bottom of the excavation is located in soft soil and the ratio of D/H in this excavation is 1.09 (>1.0). At excavation V, the ratio of D/H is 0.71 (<1.0). The increment of lateral displacement takes place mainly when the ratio of D/H is more than 1.0. The beneficial influence of bedrock becomes significant when D/H is less than 1.0.

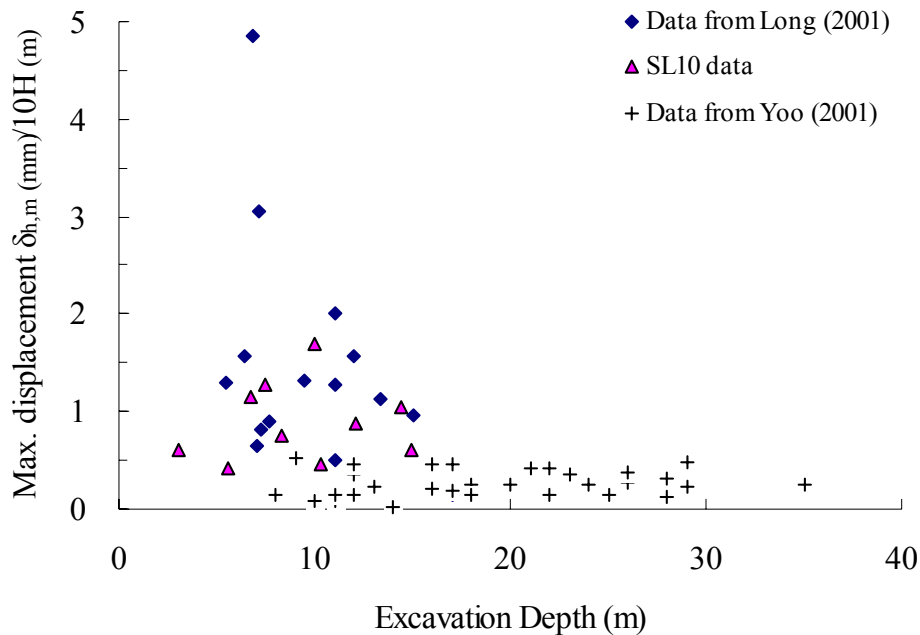


Figure 18. Variation of $\delta_{h,m}/H$ with excavation depth.

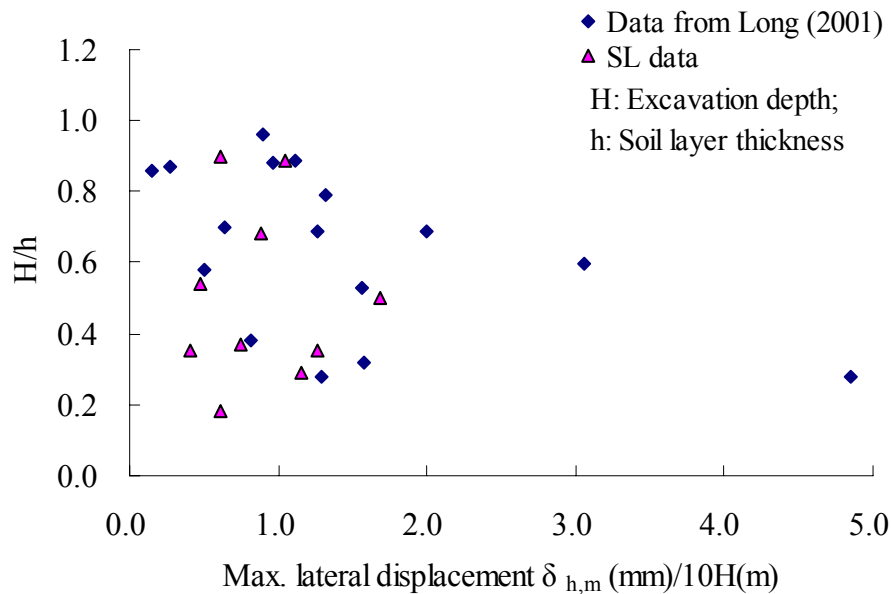


Figure 19. H/h versus normalized maximum displacement.

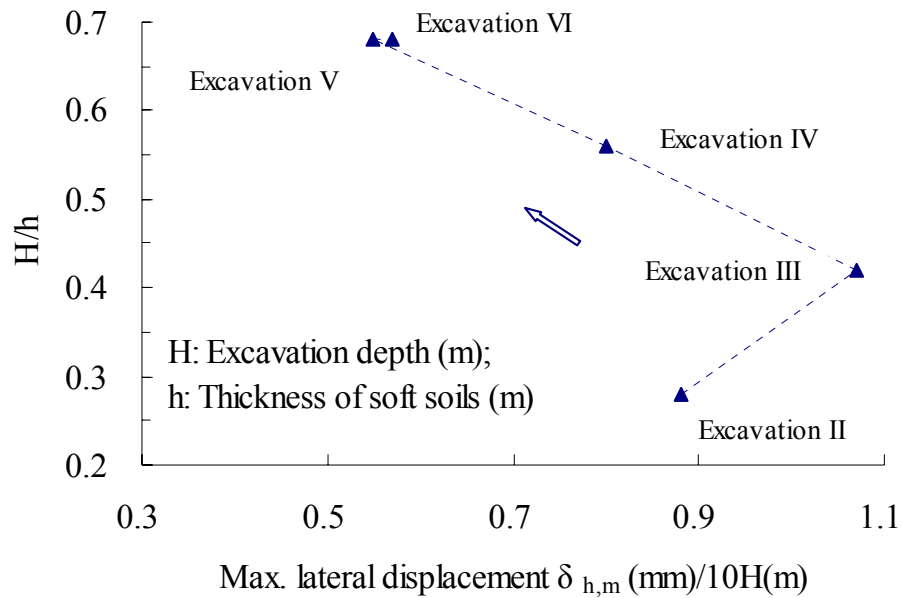


Figure 20. H/h versus normalized displacement in stages.

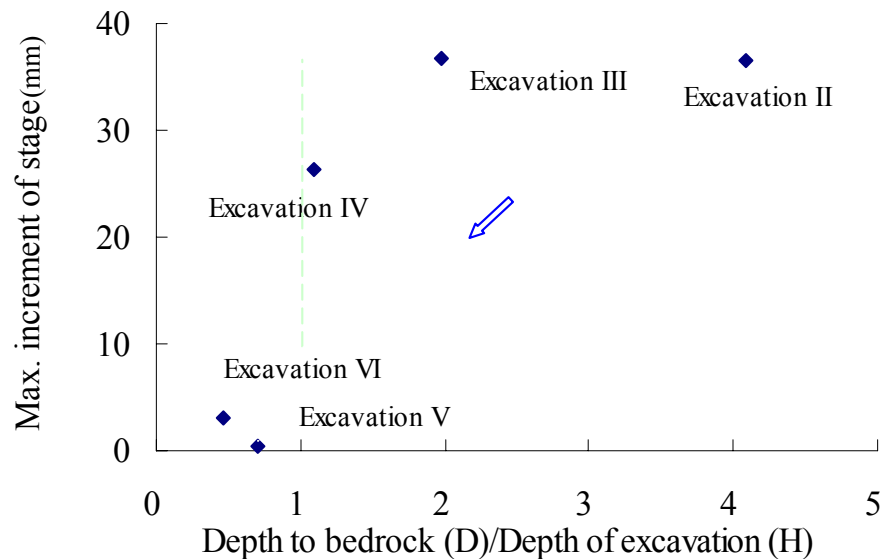


Figure 21. Maximum displacement increment versus D/H in stages.

Effect of System Stiffness

The effect of system stiffness for a propped retaining wall system on the maximum lateral deformation has been a subject for deep excavation projects in soft soil. Since Rowe (1952) studied this problem with structural engineering principles, different definitions for wall system stiffness have been developed by others, such as Goldberg et al. (1976), Mana and Clough (1981), and Clough et al. (1989). More recently, Yoo and Lee (2008), using numerical methods, investigated the effects of wall stiffness, unsupported depth, and soil stiffness on the wall and ground movement characteristics at deep excavations. The combination effect of the parameters of wall stiffness, unsupported depth, and soil stiffness was presented in terms of a flexibility ratio



$$F \approx \frac{E_s L^3}{EI} \quad (1)$$

where E_s is the soil stiffness, L is the unsupported excavation length below the last support, and EI is the wall flexural rigidity. Yoo and Lee (2008) showed that L and over-excavation have a greater influence on the wall deformations of a given excavation than EI does.

For the excavations at SL10, the wall stiffness (EI) is same with depth in a section. The undrained shear strength of the soft clay is almost the same in the upper part and increases with depth in a magnitude of 2 kN/m^2 in the lower part. The stiffness E_s of soil is correlated to its undrained shear strength. The soil stiffness E_s at the SL10 can be generally considered the same in a section or increasing by 10% per meter depth. The vertical intervals of anchors vary from 1.5 m to 3.0 m at SL10. However, for the sections where the excavation occurs in soft clay, the vertical intervals of anchors are 2.0 m to 2.5 m in the middle and lower parts of a section. The unsupported excavation lengths below the last support (L) in these sections were strictly controlled in accordance to the vertical intervals of anchors, as illustrated in Figure 4. So, the influence of the unsupported length below the last support L on the wall deformations at SL10 should be insignificant.

For a sheet pile wall-anchor system, another definition of system stiffness, $k_s = EI/(\gamma_w h_{\text{avg}}^4)$ is also well accepted, where γ_w is the unit weight of water and h_{avg} is the average vertical spacing of the anchors, E is Young's modulus of the wall, and I is the structural internal moment of inertia per unit length of the wall.

Yoo (2001) reviewed data from Korea, where deep excavation is conducted in soft soil overlying bedrock under the support of a propped retaining wall system. The result shows that there is a boundary line and most of the data are plotted into the area below this line, as shown in Figure 22. The boundary line follows an exponential decay function and is described as $0.1\delta_{h,m}/H = 0.5\exp(-0.007k_s)$ (Yoo, 2001). Data from Yoo (2001) indicate that the maximum lateral deformation of a sheet pile wall system should decrease as its system stiffness k_s increases.

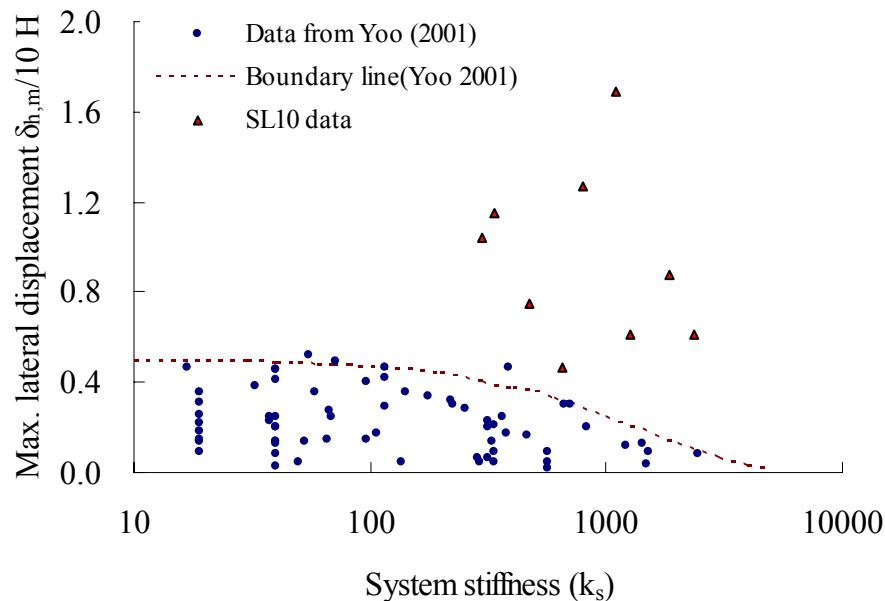


Figure 22. Variation of normalized displacement with support stiffness.

Figure 22 shows the variation of maximum lateral wall movements $0.1\delta_{h,m}/H$ with the system stiffness k_s for the measured data from SL10 together with the data from Yoo (2001). It is evident that the data from SL10 is far above the boundary line $0.1\delta_{h,m}/H = 0.5\exp(-0.007k_s)$ and that the deformation magnitude of SL10 is different from the Korea cases. There is no clear relationship in the data from SL 10, which shows that the normalized lateral deformation $0.1\delta_{h,m}/H$ varies heavily depending on the system stiffness k_s .



As can be seen in Figure 22, there is greater scatter in system stiffness data for SL 10 than for the Korea cases. This implies that the lateral displacements in SL10 are more prone to site conditions such as ground water, retained soil stiffness, and workmanship. A possible explanation for the lack of dependency on system stiffness is that once sufficient stiffness is available, movement is determined by the magnitude of the excavation base heave, and also whether or not the soil has significant “self support” capacity (Long, 2001).

Figure 22 shows that the system stiffness of a sheet pile wall system is not a key factor influencing its deformation, once certain wall stiffness is conditioned. The trend of the data in Figure 18 indicates that the normalized lateral displacement tends to decrease with increasing excavation depth, suggesting a greater degree of control on the lateral displacement by soft soil conditions at dredge level.

For section 1/840N, Figure 23 shows that the system stiffness increases generally from excavations II through VI, which corresponds with the decrease of the maximum increment of lateral displacement for excavations. Since the larger lateral displacement increments are in excavations II and III (the largest displacement taking place in excavation III), decreasing the distance of the first three anchor levels could prove to be an effective way to lessen lateral displacement. For a wall with less stiffness, the maximum wall bending moment will be effectively reduced. Potts and Day (1990) showed that if the increased movements, associated with more flexible walls, can be accommodated or reduced by extra propping, such walls can provide economic and viable solutions.

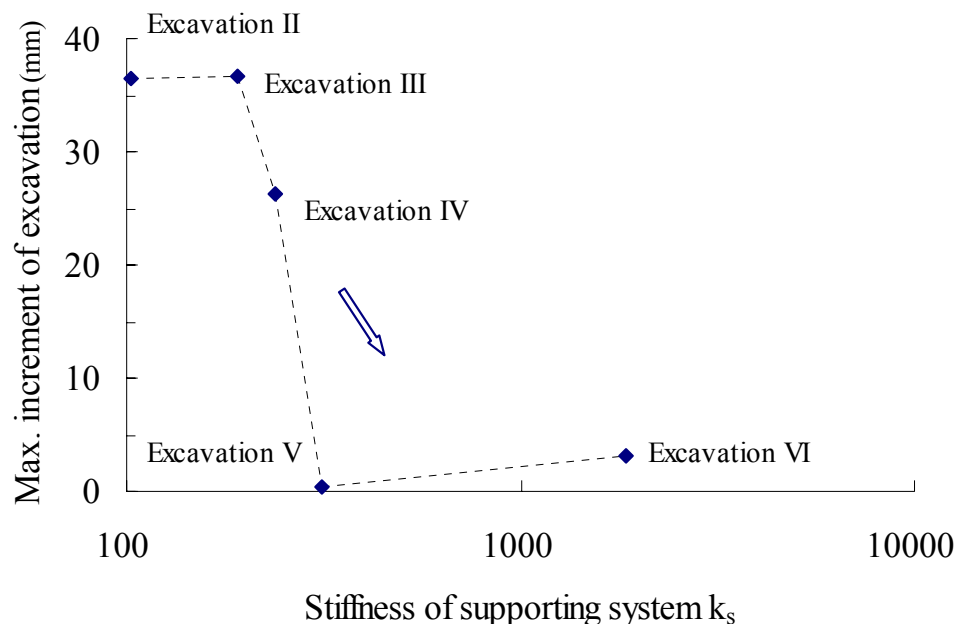


Figure 23. Variation of the maximum displacement increment with support system stiffness.

The Influence of Soil Strength

It is well accepted that the deformation feature of the wall-prop system varies depending heavily on the properties of the soil layer. In order to properly make comparison between the current study and the other case studies, the ground conditions should be thoroughly compared. Unfortunately, it is impossible to compare the soil parameters of SL10 with the cases from Long (2001) and Yoo (2001) in detail since the parameters have only been partially shown. However, the general comparison shows that the soil strength of the cases from Yoo (2001) is higher than that of both SL10 and the cases from Long (2001).

It is noted that the case histories from Yoo (2001) are mostly related to alluvial, residual soil layers and weathered rock overlying bedrock. There are differences in the geotechnical conditions of the case from Yoo (2001) and SL10. Their geotechnical conditions are compared in Table 3.



Table 3. Comparison of the cases of deep excavation in soft soil overlying bedrock.

Case	Cases from Korea (Yoo 2001)		South Link 10 in Stockholm	
	Layers	Thickness (m)*	Layers	Thickness (m)
Geotechnical conditions	Fill	1.5	Fill	1.0
	Weathered soil	1.5	Dry crust	1.0
	Residual soil	8.5	Soft clay	13-20
	Weathered rock	13.0	Granular soil	1.0 m
	Hard rock	Great depth	Hard rock	Great depth
Formation level	Residual soil or rock		Soft clay	
Ratio of h^{**}/H	$h \approx 0.3H$ to $1.0 H$		$h > 1.1H$	
Bedrock	Hard rock		Hard rock	

* the estimated thickness.

** h: the total thickness of soft soil, fill, and dry crust layers; H: the depth of excavations.

The strength of the soft clay at SL10 is lower than that of the residual soils of Yoo (2001). For the soft clay in Sweden, when the effective stresses thrusting on the soft soil are more than half of the soil pre-stresses in geological history, the magnitude of the soil deformation is generally beyond that of a project's limiting criteria. For normally consolidated or slightly overconsolidated soft clay, the pre-stress in geological history is so small that it is easily exceeded provided the ground movement is not properly controlled. In practice, the undrained shear strength, which can be mobilized for a project, is generally approximated by an inertial friction angle ϕ less than 16° or even $\phi = 0$ (Larsson, 1977; 1986).

The parameters used by Yoo (2001) to simulate the behavior of the wall-retained soil system in a numerical model are different from those of SL10. The value of ϕ for the soil in the Yoo (2001) model is 42° , which is greater than the 16° used for the soil at SL10. The strength of the residual soil in Yoo's model is greater than that of the soft clay of SL10.

For the case with $h > H$ from Long (2001), there is only undrained strength c_u available. The soft soil strength varies from 10 to 50 kPa and averages around 20 kPa, which is similar to the clay strength of SL10.

Following Clough et al. (1989), the influence of the soil strength on the stability of the excavation bottom is shown in Figure 24. Figure 24 shows that the data from Yoo (2001) is in line with the general conclusion that the lateral displacement of a wall decreases with higher factor of safety (FOS) at excavation base and higher system stiffness, while the data from SL10 and Long (2001) is not. The data from SL10 and Long (2001) is around or above the line of $FOS = 1.1$. Even in the data from Yoo (2001), some points lie around or above the line of $FOS = 2.0$, which means that the factors of safety of the excavation bottom of the related excavations are less than 2.0. This indicates that FOS should not be a key factor for the design of a deep excavation in soft soils overlying rock or a stiff layer. However, the lower FOS of SL10 and Long (2001) corresponding to larger displacements shown in Figure 24 indicate that the larger lateral deformation in SL10 should, at least partially, be contributed to the lower soil strength.

It is noted that the parameter FOS only refers to base stability, as highlighted in Figure 24. For deep excavations in soft soils, the vertical movements may be translated to horizontal movements, resulting in larger lateral wall movement. As the excavation bottom gets near to bedrock, the presence of the bedrock will prevent a deeper flow of soft soil (which contrasts situations where bedrock is not present). The lateral displacement increasing feature of test section 1/840N (figs. 10 and 11) indicates the bedrock's beneficial effect of preventing a deeper flow of soft soils as the excavation bottom nears bedrock. Where the depth of the excavation bottom to bedrock (D) is large enough (i.e., $H/D > 1.0$), a reasonable factor of safety is still necessary for an excavation. The comparable lateral displacement and soil strength between the case of $h > H$ from Long (2001) and SL10 support this deduction.

More recently, Moormann (2004) concluded that ground conditions were identified as one of the most influential parameters. The maximum lateral and vertical movements due to deep excavation in cohesive soils of very soft to soft consistency, with undrained shear strength $c_u < 75 \text{ kN/m}^2$, can be more than 1% of H, the excavation depth, and the ratio of the maximum surface settlement to the maximum lateral displacement can be as high as 2.0. The magnitude of the movement in SL10 falls in this varying range.

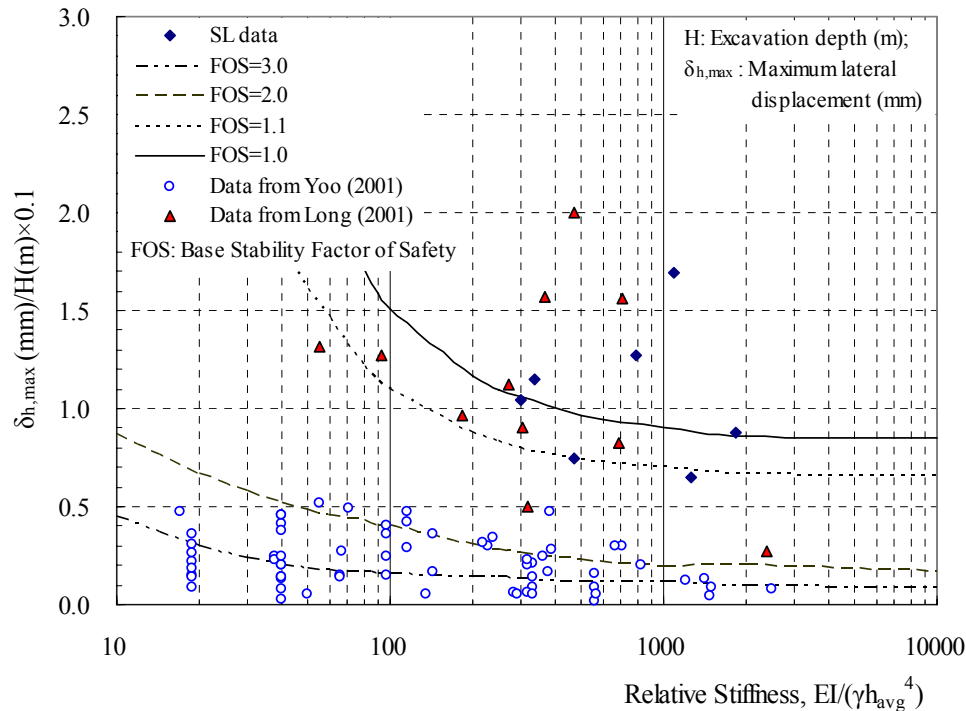


Figure 24. Maximum lateral displacement versus system stiffness and base stability factor of safety.

CONCLUSION

This study examines the measured data concerning ground and wall movements at deep excavations in soft soils overlying rock in contractor SL10 in Stockholm. Attention has been paid to the features of the lateral wall movements. Based on this study, the following conclusions can be drawn:

1. Mainly due to the low strength of the soft soil at the excavations and the excavation formation levels being in soft soil in South Link 10, the lateral wall deformations for the sheet pile walls in South Link 10 are larger than those of the walls in other similar cases, where walls are also keyed into rock or stiff soil with their formation level in rock or in soft soil.
2. The magnitude of the lateral displacement in SL 10 varies widely from 0.4% to 1.7% H, where H is excavation depth. The lateral displacement is about 40% to 125% the magnitude of the maximum surface settlement. The beneficial effect of the bedrock should be carefully considered for estimating the movements of the walls in soft soils with strength as low as that of SL10.
3. The data of both monitored and numerical analyses from test section 1/840N show that the displacement of the walls mainly takes place in the first three excavation stages, though the displacement in the first excavation stage is not completely measured in practice.
4. Of the parameters effecting the lateral deformation of the walls in SL10, the properties of the retained soil and the ratio of excavation depth (H) to depth of the excavation bottom to bedrock (D) are the most prominent factors determining whether or not the retaining capacity of the wall is adequate. The influence of the bedrock is overshadowed by the low strength of the soils, where D is larger than H (i.e., $D/H > 1.0$).
5. There is no clear evidence that lateral displacement can be effectively reduced by merely increasing the wall system stiffness k_s (Clough et al., 1989) in SL10. However, the lateral displacement increasing feature in section 1/840N implies that decreasing the vertical space of the anchor levels in the upper part of an excavation could be an effective way to decrease lateral displacement.



ACKNOWLEDGMENTS

The authors would like to thank Professor Devendra Narain Singh for his technical suggestions and three anonymous reviewers for their constructive review comments.

REFERENCES

- Bergdahl, U., Larsson, R. and Viberg, L. (2003). "Ground investigations and parameter assessment for different geological deposits in Sweden." In-Situ Characterization of Soils. K.R. Saxena and V.M. Sharma, ed., A.A. Balkema Publishers, India, 119-170.
- Bjerrum, L., Clausen, C.J., and Duncan, J.M. (1972). "Earth pressures on flexible structures (a state-of-the-art report)." Proc. 5th European Conf. on Soil Mech. and Found. Engrg., Madrid, Spain, Vol.2, 169-196.
- Brinkgreve, R.B.J. (Ed) (2002). "PLAXIS - Finite Element Code for Soil and Rock Analyses: Users Manual -Version 8." A.A. Balkema, Rotterdam, Netherlands.
- Clough, G.W. and O'Rourke, T.D. (1990). "Construction induced movements of in situ walls." Proc. on Conf. on Design and Performance of Earth Retaining Structures, ASCE, Geotechnical Special Publication No. 25, 439-470.
- Clough, G.W., Smith, E.M., and Sweeney, B.P. (1989). "Movement control of excavation support system by iterative design." Foundation Engineering, Current Practices and Principles, Geotechnical Special Publication 22, F.H. Kulhawy, ed., ASCE, Vol.2, 869-884.
- Finno, R.J. and Calvello, M. (2005). "Supported Excavations: the Observational Method and Inverse Modeling." J. Geotech. and Geoenviron. Engrg., Vol.131(7), 826-836.
- Goldberg, D. T., Jaworski, W. E., and Gordon, M. D. (1976). "Lateral support systems and underpinning, construction methods." Rep.FHWA-RD-75-128, 129 and 130, Federal Highway Administration, Washington, D.C.
- Hashash, Y. M. A., and Whittle, A. J.(1996). "Ground movement prediction for deep excavations in soft clay." J. Geotech. Engrg., Vol.122(6), 474-486.
- Hashash, Y.M.A. and Whittle, A.J. (2002). "Mechanisms of load transfer and arching for braced excavations in clay." J. Geotech. and Geoenviron. Engrg., Vol.128(3), 187-197.
- Hintze, S., Ekenberg, M. and Holmberg, G. (2000). "Southern Link Road Construction: Foundation and Temporary Constructions." Proc. 16th IABSE Congress, CD-ROM, Lucerne, Switzerland.
- Hsieh, P.G. and Ou, C.Y. (1998). "Shape of ground surface settlement profiles caused by excavation." Can. Geotech. J., Vol.35(6), 1004-1017.
- Larsson, R. (1977). "Basic Behaviour of Scandinavian Soft Clays." Swedish Geotechnical Institute, Report No.4, Linköping.
- Larsson, R., Bergdahl, U., and Eriksson, L. (1984). "Evaluation of shear strength in cohesive soils with special reference to Swedish practice and experience." Swedish Geotechnical Institute (SGI), Information No. 3E, Linköping.
- Larsson, R. (1986). " Consolidation of soft soils." Swedish Geotechnical Institute, Report No.29, Linköping.
- Larsson, R. and Mulabdić, M. (1991). " Shear Moduli in Scandinavian Clays -Measurement of initial shear modulus with seismic cones/- Empirical correlations for the initial shear modulus in clay." Swedish Geotechnical Institute, Report No.40, Linköping.
- Long, M. (2001). "Database for Retaining Wall and Ground Movements due to Deep Excavations." J. Geotech. and Geoenviron. Engrg., Vol.127(2), 203-224.
- Ma, J.Q., Berggren, B.S., Bengtsson, P.E., Stille, H. and Hintze, S. (2006). "Back analysis on a deep excavation in Stockholm with finite element method." Proc. 6th European Conference on Numerical Methods in Geotechnical Engineering, Graz, Austria, 423-429.
- Mana, A.I. and Clough, G.W. (1981). "Prediction of movements for braced cuts in clay." J. Geotech. Engrg., Vol.107(6), 759-777.
- Mayne, P.W. and Kulhawy, F.H. (1982). "K₀-OCR Relationships in Soil." J. Geotech Engrg., Vol.108(6), 851-872.
- Moormann, C.(2004). "Analysis of Wall and Ground Movements due to Deep Excavations in Soft Soil Based on a New Worldwide Database." Soils and Foundations, Vol.44 (1), 87-98.
- Ou, C.Y., Hsieh, P.O. and Chiou, D.C. (1993). "Characteristics of ground surface settlement during excavation." Can. Geotech. J., Vol.30(5), 758-767.
- Peck, R. B. (1969). "Deep excavations and tunneling in soft ground". Proc., 7th Int. Conf. on Soil Mech. and Found. Engrg., State-of-the-Art Rep., 225-290.
- Shao, Y. and Macari, E.J. (2008). "Information Feedback Analysis in Deep Excavations." International Journal of Geomechanics, Vol. 8(1): 91-103.



-
- Wong, I.H., Poh, T.Y. and Chuah, H.L. (1997). "Performance of Excavations for Depressed Expressway in Singapore." J. Geotech. and Geoenviron. Engrg., Vol.123(7), 617-625.
- Yoo, C.S. (2001). "Behavior of braced and anchored walls in soils overlying rock." J. Geotech. and Geoenviron. Engrg., Vol. 127(3), 225-233.
- Yoo, C.S. and Lee, D.Y. (2008). "Deep excavation-induced ground surface movement characteristics – A numerical investigation." Computers and Geotechnics, Vol.35, 231–252.

NOTATIONS

c_u - undrained shear strength of soil

D - depth of the excavation bottom to bedrock

E - Young's modulus of the wall

EI - wall flexural rigidity

E_s - soil stiffness

$$F \approx \frac{E_s L^3}{EI}$$

F - flexibility ratio being approximated as:

FOS - factor of safety at excavation base

H - excavation depth

h - thickness of soft soil at an excavation

h_{avg} - average vertical spacing of the anchors

I - structural internal moment of inertia per unit length of the wall

k_0 - lateral coefficient value of retained soils at rest

k_s - wall system stiffness, $k_s = EI/(\gamma_w h_{avg}^4)$

L - unsupported excavation length below the last support

OCR - overconsolidation ratio

SL10 - South Link 10

γ_w - unit weight of water

$\delta_{h,m}$ - maximum lateral displacement

$\delta_{v,m}$ - maximum settlement

ϕ - inertial friction angle of soil



INTERNATIONAL JOURNAL OF
**GEOENGINEERING
CASE HISTORIES**

*The Journal's Open Access Mission is
generously supported by the following Organizations:*



Access the content of the *ISSMGE International Journal of Geotechnical Engineering Case Histories* at:
www.geocasehistoriesjournal.org